Adv Comput Math (2017) 43:1197–1225
DOI 10.1007/s10444-017-9521-4

A well-balanced van Leer-type numerical scheme for shallow water equations with variable topography

Dao Huy Cuong[1,3] · **Mai Duc Thanh**[2]

Received: 20 February 2016 / Accepted: 7 February 2017 /
Published online: 23 February 2017

Abstract A well-balanced van Leer-type numerical scheme for the shallow water equations with variable topography is presented. The model involves a nonconservative term, which often makes standard schemes difficult to approximate solutions in certain regions. The construction of our scheme is based on exact solutions in computational form of local Riemann problems. Numerical tests are conducted, where comparisons between this van Leer-type scheme and a Godunov-type scheme are provided. Data for the tests are taken in both the subcritical region as well as supercritical region. Especially, tests for resonant cases where the exact solutions contain coinciding waves are also investigated. All numerical tests show that each of these two methods can give a good accuracy, while the van Leer -type scheme gives a better accuracy than the Godunov-type scheme. Furthermore, it is shown that the van Leer-type scheme is also well-balanced in the sense that it can capture exactly stationary contact discontinuity waves.

Keywords Shallow water equations · Resonant · Nonconservative · Riemann problem · Godunov scheme · Van Leer scheme · Accuracy

Communicated by: Leslie Greengard

✉ Mai Duc Thanh
mdthanh@hcmiu.edu.vn

Dao Huy Cuong
cuongnhc82@gmail.com

[1] Nguyen Huu Cau High School, 07 Nguyen Anh Thu str., Trung Chanh Ward, Hoc Mon District, Ho Chi Minh City, Vietnam

[2] Department of Mathematics, International University, Vietnam National University-Ho Chi Minh City, Quarter 6, Linh Trung Ward, Thu Duc District, Ho Chi Minh City, Vietnam

[3] Department of Mathematics and Computer Science, University of Science, Vietnam National University-Ho Chi Minh City, 227 Nguyen Van Cu str., District 5, Ho Chi Minh City, Vietnam

1 Introduction

In this paper we will construct a van Leer - type scheme for the following shallow water equations with variable topography

$$\begin{aligned} &\partial_t h + \partial_x (hu) = 0, \\ &\partial_t (hu) + \partial_x \left(h \left(u^2 + \frac{gh}{2} \right) \right) = -gh\partial_x a, \end{aligned} \tag{1.1}$$

where the height of the water from the bottom to the surface, denoted by h, and the fluid velocity u are the main unknowns. Here, g is the gravity constant, and $a = a(x)$ (with $x \in \mathbb{R}$) is the height of the bottom from a given level.

The system (1.1) has a source term on the right-hand side. By supplementing the system (1.1) with the following trivial equation (see [24, 25]),

$$\partial_t a = 0, \tag{1.2}$$

one can reduce it into a system of balance laws in nonconservative form. Weak solutions of this kind of systems can be understood in the sense of *nonconservative products*, see [12]. Often, nonconservative terms cause lots of inconveniences for standard numerical schemes. Study of systems of balance laws in nonconservative form has been a very intensive and challenging topic for many authors during the past decades.

Recently, a Godunov-type scheme for Eq. 1.1 was constructed and tested in [28], where most tests show that the Godunov-type scheme can provide good approximations of the solutions. However, an error in the programming makes the scheme fail to approximate the exact solution in a resonant case in [28]. Since van Leer's scheme for hyperbolic systems of conservation laws can improve the accuracy of the Godunov scheme, we are motivated to study a van Leer-type scheme for the nonconservative system (1.1). As the Godunov-type scheme, this van Leer-type scheme is based on exact solutions of local Riemann problems at each grid cell. Then, we will show that the van Leer-type scheme is well-balanced in the sense that it can capture exactly stationary discontinuity waves. Numerical tests are then conducted in all the cases, where the initial data may belong to the subcritical region, or supercritical region, or both kinds of regions. In particular, we present tests for the resonant cases where the initial data belong to both subcritical and supercritical regions. In each of these tests, we compute the errors for the Godunov-type and van Leer-type schemes. It is shown that the error goes to zero as the mesh size goes to zero, and the errors for van Leer-type scheme are much smaller than the ones of the Godunov-type scheme in all the tests. Thus, both van Leer-type scheme and Godunov-type scheme can provide convergent approximate solutions to the exact solutions, even in the resonant cases. Moreover, the van Leer-type scheme gives a better accuracy than the Godunov-type scheme.

There have been many works in the literature for the study of numerical approximations of shallow water equations and nonconservative systems, see [7, 13, 15, 17, 18, 30]. Godunov-type schemes for hyperbolic systems of balance laws in nonconservative forms are considered in [2, 9, 28, 31, 32]. The Riemann problem for shallow water equations were studied in [27, 28]. The Riemann problem for other

hyperbolic systems in nonconservative form were considered in [16, 19–21, 26, 29, 34–36]. Well-balanced numerical schemes for a single conservation law with source term were studied in [3, 5, 6]. Well-balanced schemes for the model of a fluid flow in a nozzle with variable cross-section were constructed in [22, 23]. Numerical schemes for two-phase flow models were presented in [1, 4, 8, 11, 33]. See also the references therein.

The organization of this paper is as follows. In Section 2 we will present basic properties of the system Eqs. 1.1–1.2. The Riemann problem is revisited in Section 3. Section 4 is devoted to the construction of the van Leer-type scheme, after a brief review of the Godunov-type scheme for Eq. 1.1. Numerical tests are given in Section 5. Finally, we draw several conclusions in Section 6.

2 Preliminaries

2.1 Wave curves

The system (1.1)–(1.2) can be re-written as a non-conservative system as

$$\partial_t U + A(U)\partial_x U = 0, \tag{2.1}$$

where

$$U := \begin{pmatrix} h \\ u \\ a \end{pmatrix}, \quad A(U) := \begin{pmatrix} u & h & 0 \\ g & u & g \\ 0 & 0 & 0 \end{pmatrix}.$$

The matrix $A = A(U)$ has three real eigenvalues

$$\lambda_1(U) := u - \sqrt{gh} < \lambda_2(U) := u + \sqrt{gh}, \quad \lambda_3(U) := 0, \tag{2.2}$$

together with the corresponding eigenvectors which can be chosen as

$$r_1(U) := \begin{pmatrix} h \\ -\sqrt{gh} \\ 0 \end{pmatrix}, \quad r_2(U) := \begin{pmatrix} h \\ \sqrt{gh} \\ 0 \end{pmatrix}, \quad r_3(U) := \begin{pmatrix} gh \\ -gu \\ u^2 - gh \end{pmatrix}. \tag{2.3}$$

The system is *strictly hyperbolic* on the domain $G_1 \cup G_2 \cup G_3$, where

$$\begin{aligned} G_1 &:= \Big\{U = (h,u,a): \quad \lambda_1 > \lambda_3\Big\} = \Big\{U = (h,u,a): \quad u > \sqrt{gh}\Big\}, \\ G_2 &:= \Big\{U = (h,u,a): \quad \lambda_2 > \lambda_3 > \lambda_1\Big\} = \Big\{U = (h,u,a): \quad |u| < \sqrt{gh}\Big\}, \\ G_3 &:= \Big\{U = (h,u,a): \quad \lambda_3 > \lambda_2\Big\} = \Big\{U = (h,u,a): \quad u < -\sqrt{gh}\Big\}. \end{aligned} \tag{2.4}$$

The first and the third characteristic speeds λ_1 and λ_3 coincide on the surface

$$\mathcal{C}^+ := \Big\{(h,u,a): \quad u = \sqrt{gh}\Big\}.$$

The second and the third characteristic speeds λ_2 and λ_3 coincide on the surface

$$\mathcal{C}^- := \Big\{(h,u,a): \quad u = -\sqrt{gh}\Big\}.$$

In water resource engineering, any state in the regions G_1 and G_2 is said to be *supercritical*, while each state in the region G_2 is said to be *subcritical*. A state on the curves $\mathcal{C}^{\pm}$ is said to be *critical*. These terminologies are corresponding to the value of the Froude number

$$Fr := \frac{|u|}{\sqrt{gh}}.$$

This means that a supercritical state is the one at which $Fr > 1$; a subcritical state is the one at which $Fr < 1$; and a critical state is the one at which $Fr = 1$.

It is easy to see that the first and second characteristic fields (λ_1, r_1), (λ_2, r_2) are genuinely non-linear, that is

$$\nabla\lambda_1 \cdot r_1 \neq 0, \quad \nabla\lambda_2 \cdot r_2 \neq 0,$$

and that the third characteristic field (λ_3, r_3) is linearly degenerate, that is

$$\nabla\lambda_3 \cdot r_3 = 0.$$

Let us recall that a *discontinuity wave* of Eqs. 1.1–1.2 is a weak solution of the form

$$U(x,t) = \begin{cases} U_- = (h_-, u_-, a_-), & x < \sigma t, \\ U_+ = (h_+, u_+, a_+), & x > \sigma t, \end{cases} \tag{2.5}$$

where U_-, U_+ are the left-hand and right-hand states, respectively, and $\sigma = \sigma(U_-, U_+)$ is the speed of the discontinuity wave.

The Rankine-Hugoniot relation associated with Eq. 1.2 takes the form

$$-\sigma[a] = 0, \tag{2.6}$$

where σ denotes the speed of the discontinuity wave, $[a] = a_+ - a_-$ is the jump of the quantity a across the discontinuity wave. Therefore, as discussed in [27], across a discontinuity wave there are two possibilities:

(i) either the bottom height a remains constant,
(ii) or the speed $\sigma = 0 = \lambda_3(U_\pm)$, so this is the 3−contact discontinuity wave, so called *the stationary contact discontinuity*, since this wave is independent of time.

Let us consider the first the case (i), where the system (1.1)–(1.2) is reduced to the usual shallow water equations with flat bottom. Then, we can determine the Rankine-Hugoniot relations and the admissibility criterion for shock waves as usual.

A shock wave (2.5) is *admissible*, called the ith-Lax shock, if it satisfies the Lax shock inequalities,

$$\lambda_i(U_+) < \sigma(U_-, U_+) < \lambda_i(U_-), \quad i = 1, 2. \tag{2.7}$$

From now on, we consider admissible shock waves, only.

Given a left-hand state U_0, the set of all right-hand states that can be connected to U_0 by 1st-Lax shock forms a curve, denoted by $\mathcal{S}_1(U_0)$. In a backward way, given

a right-hand state U_0, the set of all left-hand states that can be connected to U_0 by 2nd-Lax shock forms a curve, denoted by $\mathcal{S}_2^B(U_0)$. These curves are defined by

$$\begin{aligned} \mathcal{S}_1(U_0): &\quad u = u_0 - \sqrt{\frac{g}{2}}(h-h_0)\sqrt{\frac{1}{h}+\frac{1}{h_0}}, \quad h > h_0, \\ \mathcal{S}_2^B(U_0): &\quad u = u_0 + \sqrt{\frac{g}{2}}(h-h_0)\sqrt{\frac{1}{h}+\frac{1}{h_0}}, \quad h > h_0, \end{aligned} \tag{2.8}$$

see [27].

It is interesting that the shock speeds in the non-linear characteristic fields may coincide with the characteristic speed of the linearly degenerate field as stated in the following lemma.

Lemma 2.1 (Lem. 2.1, [28]) *Consider the projection of the wave curves on the (h,u)-plan. To every $U_L = (h_L, u_L) \in G_1$ there exists exactly one point $U^\# \in S_1(U_L) \cap G_2^+$ such that the $1-$shock speed $\sigma_1(U_L, U^\#) = 0$. The state $U^\# = (h^\#, u^\#)$ is defined by*

$$h^\# = \frac{-h_L + \sqrt{h_L^2 + 8h_L u_L^2/g}}{2}, \quad u^\# = \frac{u_L h_L}{h^\#}.$$

Moreover, for any $U \in \mathcal{S}_1(U_L)$, the shock speed $\sigma_1(U_L, U) > 0$ if and only if U is located above $U^\#$ on $\mathcal{S}_1(U_L)$.

Next, let us consider rarefaction waves, which are piecewise smooth self-similar solutions of Eqs. 1.1–1.2, i.e.

$$U(x,t) = V(\xi), \quad \xi = \frac{x}{t}, \quad x \in \mathbb{R}, t > 0.$$

Substituting this into Eq. 2.1, we can see that rarefaction waves are solutions of the following initial-value problem for ordinary differential equations

$$\begin{aligned} &\frac{dV(\xi)}{d\xi} = r_j(V(\xi)), \quad \xi \geq \lambda_j(U_0), \\ &V(\lambda_j(U_0)) = U_0, \quad j = 1, 2, \end{aligned} \tag{2.9}$$

where the eigenvectors r_1 and r_2 are given by Eq. 2.3. In particular, it holds along the integral curves that

$$\frac{da(\xi)}{d\xi} = 0,$$

which means that the bottom height a remains constant through any rarefaction fan.

Given a left-hand state U_0, the set of all right-hand states that can be connected to U_0 by 1-rarefaction wave of Eqs. 1.1–1.2 forms a curve, denoted by $\mathcal{R}_1(U_0)$. In a backward way, given a right-hand state U_0, the set of all left-hand states that can be connected to U_0 by 2-rarefaction wave forms a curve, denoted by $\mathcal{R}_2^B(U_0)$. These curves are given by

$$\begin{aligned} \mathcal{R}_1(U_0): &\quad u = u_0 - 2\sqrt{g}(\sqrt{h} - \sqrt{h_0}), \quad h \leq h_0, \\ \mathcal{R}_2^B(U_0): &\quad u = u_0 + 2\sqrt{g}(\sqrt{h} - \sqrt{h_0}), \quad h \leq h_0, \end{aligned} \tag{2.10}$$

see [27]. We can therefore define the forward and backward wave curves in the non-linear characteristic fields as follows

$$\begin{aligned} \mathcal{W}_1(U_0) &= \mathcal{R}_1(U_0) \cup \mathcal{S}_1(U_0), \\ \mathcal{W}_2^B(U_0) &= \mathcal{R}_2^B(U_0) \cup \mathcal{S}_2^B(U_0). \end{aligned} \tag{2.11}$$

As seen above, the curves $\mathcal{W}_1(U_0)$ can be parameterized as a function $u = w_1(U_0; h)$ of $h > 0$, and the curves $\mathcal{W}_2^B(U_0)$ can be parameterized as a function $u = w_2^B(U_0; h)$ of $h > 0$. It was shown in [27] that $w_1(U_0; h)$ is strictly convex and strictly decreasing functions of $h > 0$, while $w_2^B(U_0; h)$ is strictly concave and strictly increasing functions of $h > 0$.

Let us now consider the case (ii), where the discontinuity satisfies the jump relations

$$\begin{aligned} [hu] &= 0, \\ \left[\frac{u^2}{2} + g(h + a)\right] &= 0. \end{aligned} \tag{2.12}$$

The last jump relations determine the stationary-wave curve (parameterized with h) as follows

$$\begin{aligned} \mathcal{W}_3(U_0) : u = w_3(U_0; h) &:= \frac{u_0 h_0}{h}, \quad h \geq 0, \\ a &= a_0 + \frac{u_0^2 - u^2}{2g} + h_0 - h. \end{aligned} \tag{2.13}$$

It is easy to check that the function $w_3(U_0; h), h \geq 0$,is strictly convex and strictly decreasing for $u_0 > 0$, and strictly concave and strictly increasing for $u_0 < 0$.

2.2 Properties of stationary contact discontinuities

Given a state $U_0 = (h_0, u_0, a_0)$ and another bottom level $a \neq a_0$, we let $U = (h, u, a)$ be the corresponding right-hand state of the stationary contact discontinuity issuing from the given left-hand state U_0. Arguing similarly as in [28], we can show that h, u can be resolved in terms of U_0, a, where h satisfies the nonlinear algebraic equation

$$2gh^3 + \Big(2g(a - a_0 - h_0) - u_0^2\Big)h^2 + h_0^2 u_0^2 = 0, \tag{2.14}$$

and u is given by

$$u = \frac{u_0 h_0}{h}. \tag{2.15}$$

Lemma 2.2 (Lem. 2.2, [28]) *Given a state $U_0 = (h_0, u_0, a_0)$ and a bottom level $a \neq a_0$. The following conclusions holds.*

(i) $a_{max}(U_0) \geq a_0$, $a_{max}(U_0) = a_0$ *if and only if* $(h_0, u_0) \in \mathcal{C}_{\pm}$.

(ii) *The non-linear equation (2.14) admits a root if and only if*

$$a \leq a_{max}(U_0) := a_0 + h_0 + \frac{u_0^2}{2g} - \frac{3}{2g^{1/3}}(h_0 u_0)^{2/3},$$

and in this case it has two roots $h_0^s \leq h_* \leq h_0^b$, which coincide only if $a = a_{max}(U_0)$.

(iii) *According to the part (ii), whenever $a \leq a_{max}(U_0)$, there are two states U_0^s, U_0^b corresponding to two roots h_0^s, h_0^b to which a stationary contact discontinuity from U_0 is possible, i.e*

$$U(x,t) = \begin{cases} U_0 = (h_0, u_0, a_0), & x < 0, \\ U_0^s = \left(h_0^s, \dfrac{h_0 u_0}{h_0^s}, a\right), & x > 0, \end{cases} \tag{2.16}$$

and

$$U(x,t) = \begin{cases} U_0 = (h_0, u_0, a_0), & x < 0, \\ U_0^b = \left(h_0^b, \dfrac{h_0 u_0}{h_0^b}, a\right), & x > 0, \end{cases} \tag{2.17}$$

are stationary contact discontinuities. Moreover, the locations of two states U_0^s, U_0^b can be determined as follows

$$\begin{aligned} &U^s \in G_1 \quad \text{if } u_0 > 0, \\ &U^s \in G_3 \quad \text{if } u_0 < 0, \\ &U^b \in G_2. \end{aligned}$$

From Lemma 2.2 , we can construct two-parameter wave sets. The Riemann problem may therefore admit up to a one-parameter family of solutions. To select a unique solution, we impose an admissibility condition, called *Monotonicity Criterion* or (MC) for short, for stationary contact discontinuities as follows

(MC) Along any stationary curve $\mathcal{W}_3(U_0)$, the bottom level a is monotone as a function of h. The total variation of the bottom level component of any Riemann solution must not exceed $|a_L - a_R|$, where a_L, a_R are left-hand and right-hand bottom levels.

A similar criterion was used in [27].

Lemma 2.3 *The Monotonicity Criterion (MC) implies that any stationary shock does not cross the boundary of strict hyperbolicity, in other words*

(i) *If $U_0 \in G_1 \cup G_3$, then only the stationary contact discontinuity U_0^s is allowed.*
(ii) *If $U_0 \in G_2$, then only the stationary contact discontinuity U_0^b is allowed.*

3 The Riemann problem revisited

Observe that by the transformation $x \mapsto -x$, $u \mapsto -u$, a left-hand (right-hand) state $U = (h, u, a)$ in G_2 (in $G_3 \cup \mathcal{C}^-$) will be transformed to the right-hand (left-hand, respectively) state $V = (h, -u, a)$ in G_2 (in $G_1 \cup \mathcal{C}^+$, respectively). Thus, the construction of wave curves and therefore the Riemann solutions for Riemann data around $\mathcal{C}^-$ can be obtained from the one for Riemann data around $\mathcal{C}^+$. Thus, without loss of generality, in the sequel we consider only the case where Riemann data are in $G_1 \cup \mathcal{C}^+ \cup G_2$.

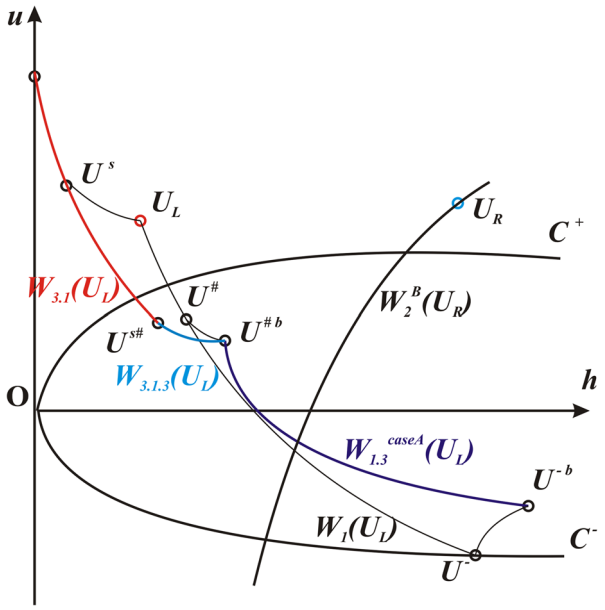

Fig. 1 The composite wave curves $\mathcal{W}_{3.1}(U_L)$, $\mathcal{W}_{3.1.3}(U_L)$ and $\mathcal{W}_{1.3}^{caseA}(U_L)$

Notations

(i) $W_k(U_i, U_j)$ ($S_k(U_i, U_j)$, $R_k(U_i, U_j)$) denotes the kth-wave (kth-shock, kth-rarefaction wave, respectively) connecting the left-hand state U_i to the right-hand state U_j, $k = 1, 2, 3$.

(ii) $W_m(U_i, U_j) \oplus W_n(U_j, U_k)$ indicates that there is an mth-wave from the left-hand state U_i to the right-hand state U_j, followed by an nth-wave from the left-hand state U_j to the right-hand state U_k, $m, n \in \{1, 2, 3\}$.

(ii) $U_0^{\#}$ denotes the state resulted by a shock wave from U_0 with zero speed.

(iv) U_0^s, U_0^b denote the states resulted by stationary contact discontinuity wave from U_0.

(v) $U^{\pm} = \mathcal{W}_1(U_L) \cap \mathcal{C}^{\pm}$.

(vi) $V_1(\xi; U_L, U_R) = \Big(h(\xi), u(\xi), a(\xi)\Big)$ denotes the $1-$rarefaction fan connecting U_L to U_R.

3.1 Case A : $U_L \in G_1 \cup \mathcal{C}^+$

Construction A1: The first part of the Riemann solution can be $W_3(U_L, U^s)$, i.e.

$$U_{exact}(x,t) = \begin{cases} U_L = (h_L, u_L, a_L), & \text{if } x/t < 0, \\ U^s = \Big(h^s, \dfrac{h_L u_L}{h^s}, a_R\Big), & \text{if } 0 < x/t < \ldots, \\ \ldots \end{cases} \tag{3.1}$$

Taking any $U \in \mathcal{R}_1(U^s)$, the second part of the solution can be $R_1(U^s, U)$, i.e.

$$U_{exact}(x,t) = \begin{cases} U_L = (h_L, u_L, a_L), & \text{if } x/t < 0, \\ U^s = \left(h^s, \dfrac{h_L u_L}{h^s}, a_R\right), & \text{if } 0 < x/t < \lambda_1(U^s), \\ V_1(x/t; U^s, U), & \text{if } \lambda_1(U^s) \le x/t \le \lambda_1(U), \\ U, & \text{if } \lambda_1(U) < x/t < \ldots, \\ \ldots \end{cases} \tag{3.2}$$

On the other hand, by Lemma 2.2, there is one state $U^{s\#} \in \mathcal{S}(U^s)$ such that the shock speed $\sigma_1(U^s, U^{s\#}) = 0$ and $\sigma_1(U^s, U) > 0$ for $h^s < h < h^{s\#}$, $\sigma_1(U^s, U) < 0$ for $h > h^{s\#}$. So, if $U \in \mathcal{S}_1(U^s)$ such that $h^s < h < h^{s\#}$, then the second part of the solution can be $S_1(U^s, U)$, i.e.

$$U_{exact}(x,t) = \begin{cases} U_L = (h_L, u_L, a_L), & \text{if } x/t < 0, \\ U^s = \left(h^s, \dfrac{h_L u_L}{h^s}, a_R\right), & \text{if } 0 < x/t < \sigma_1(U^s, U), \\ U, & \text{if } \sigma_1(U^s, U) < x/t < \ldots, \\ \ldots \end{cases} \tag{3.3}$$

Thus, if $U \in \mathcal{W}_1(U^s)$ such that $0 < h < h^{s\#}$ then first two parts of the Riemann solution are

$$W_3(U_L, U^s) \oplus W_1(U^s, U),$$

as Eqs. 3.2 or 3.3. Therefore, we call the set

$$\{U \in \mathcal{W}_1(U^s) : \quad 0 < h < h^{s\#}\} \tag{3.4}$$

as *the composite wave curve* $\mathcal{W}_{3.1}(U_L)$.

If the curve $\mathcal{W}_2^B(U_R)$ intersects the curve $\mathcal{W}_{3.1}(U_L)$ at a point U_1, then the Riemann problem of Eqs. 1.1–1.2 admits a solution of the form

$$W_3(U_L, U^s) \oplus W_1(U^s, U_1) \oplus W_2(U_1, U_R). \tag{3.5}$$

Construction A2: For each level a between a_L and a_R, the first part of the Riemann solution can be $W_3(U_L, U^s)$, where $U^s = \left(h^s, \dfrac{h_L u_L}{h^s}, a\right)$. The second part of the solution can be $S_1(U^s, U^{s\#})$. The third part of the solution can be $W_3(U^{s\#}, U^{s\#b})$, where $U^{s\#b} = \left(h^{s\#b}, u^{s\#b}, a_R\right)$. Since these three parts are discontinuity waves with same zero speed, we have a wave collision (resonant case), i.e.

$$U_{exact}(x,t) = \begin{cases} U_L = (h_L, u_L, a_L), & \text{if } x/t < 0, \\ U^{s\#b}, & \text{if } 0 < x/t < \ldots, \\ \ldots \end{cases} \tag{3.6}$$

Thus, for each level a between a_L and a_R, first three parts of the solution can be

$$W_3(U_L, U^s) \oplus S_1(U^s, U^{s\#}) \oplus W_3(U^{s\#}, U^{s\#b}),$$

as Eq. 3.6. Therefore, the set

$$\{U^{s\#b}: \quad a \text{varies between } a_L \text{ and } a_R\} \tag{3.7}$$

is called *the composite wave curve* $\mathcal{W}_{3.1.3}(U_L)$. We can check that $U^{\#b}$ and $U^{s\#}$ are two endpoints of this curve.

If the curve $\mathcal{W}_2^B(U_R)$ intersects the curve $\mathcal{W}_{3.1.3}(U_L)$ at a point U_1, then the Riemann problem of Eqs. 1.1–1.2 admits a solution of the form

$$W_3(U_L, U^s) \oplus S_1(U^s, U^{s\#}) \oplus W_3(U^{s\#}, U_1 = U^{s\#b}) \oplus W_2(U_1, U_R). \tag{3.8}$$

Construction A3: The first part of the Riemann solution can be $S_1(U_L, U_1)$, where $U_1 \in \mathcal{S}_1(U_L) \cap G_2$ such that $\sigma_1(U_L, U_1) < 0$, i.e.

$$U_{exact}(x,t) = \begin{cases} U_L = (h_L, u_L, a_L), & \text{if } x/t < \sigma_1(U_L, U_1), \\ U_1 = (h_1, u_1, a_L), & \text{if } \sigma_1(U_L, U_1) < x/t < \ldots, \\ \ldots \end{cases} \tag{3.9}$$

So, U_1 is located between $U^{\#}$ and U^- on the curve $\mathcal{S}_1(U_L)$. The second part of the solution can be $W_3(U_1, U_1^b)$, i.e.

$$U_{exact}(x,t) = \begin{cases} U_L = (h_L, u_L, a_L), & \text{if } x/t < \sigma_1(U_L, U_1), \\ U_1 = (h_1, u_1, a_L), & \text{if } \sigma_1(U_L, U_1) < x/t < 0, \\ U_1^b = (h_1^b, u_1^b, a_R), & \text{if } 0 < x/t < \ldots, \\ \ldots \end{cases} \tag{3.10}$$

Thus, for each $U_1 \in \mathcal{S}_1(U_L) \cap G_2$ such that $\sigma_1(U_L, U_1) < 0$, first two parts of the solution can be

$$S_1(U_L, U_1) \oplus W_3(U_1, U_1^b),$$

as Eq. 3.10. So, we call the set

$$\{U_1^b: \quad U_1 \in \mathcal{S}_1(U_L) \cap G_2, \sigma_1(U_L, U_1) < 0\} \tag{3.11}$$

as *the composite wave curve* $\mathcal{W}_{1.3}^{caseA}(U_L)$. Observe that $U^{\#b}$ and U^{-b} are two endpoints of this curve.

If the curve $\mathcal{W}_2^B(U_R)$ intersects the curve $\mathcal{W}_{1.3}^{caseA}(U_L)$ at a point U_2, then the Riemann problem of Eqs. 1.1–1.2 admits a solution of the form

$$S_1(U_L, U_1) \oplus W_3(U_1, U_2 = U_1^b) \oplus W_2(U_2, U_R). \tag{3.12}$$

Figure 1 illustrates the composite wave curves $\mathcal{W}_{3.1}(U_L)$, $\mathcal{W}_{3.1.3}(U_L)$ and $\mathcal{W}_{1.3}^{caseA}(U_L)$.

3.2 Case B: $U_L \in G_2$

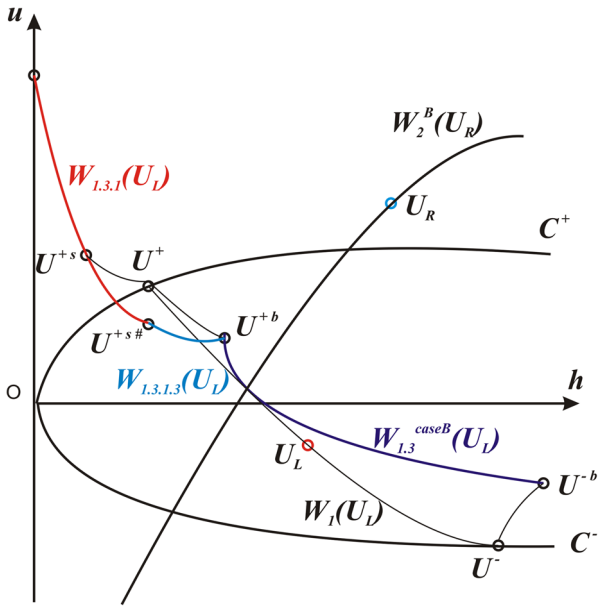

Fig. 2 The composite wave curves $\mathcal{W}_{1.3.1}(U_L)$, $\mathcal{W}_{1.3.1.3}(U_L)$ and $\mathcal{W}_{1.3}^{caseB}(U_L)$

Construction B1: The first part of the Riemann solution can be $R_1(U_L, U^+)$, i.e.

$$U_{exact}(x,t) = \begin{cases} U_L = (h_L, u_L, a_L), & if\ x/t < \lambda_1(U_L), \\ V_1(x/t; U_L, U^+), & if\ \lambda_1(U_L) \le x/t \le \lambda_1(U^+) = 0, \\ U^+ = (h^+, u^+, a_L), & if\ 0 < x/t < \ldots, \\ \ldots \end{cases} \tag{3.13}$$

The second part of the Riemann solution can be $W_3(U^+, U^{+s})$, where $U^{+s} = (h^{+s}, u^{+s}, a_R)$, i.e.

$$U_{exact}(x,t) = \begin{cases} U_L = (h_L, u_L, a_L), & if\ x/t < \lambda_1(U_L), \\ V_1(x/t; U_L, U^+), & if\ \lambda_1(U_L) \le x/t \le \lambda_1(U^+) = 0, \\ U^{+s} = (h^{+s}, u^{+s}, a_R), & if\ 0 < x/t < \ldots, \\ \ldots \end{cases} \tag{3.14}$$

Taking any $U \in \mathcal{R}_1(U^{+s})$, the third part of the solution can be $R_1(U^{+s}, U)$, i.e.

$$U_{exact}(x,t) = \begin{cases} U_L = (h_L, u_L, a_L), & if\ x/t < \lambda_1(U_L), \\ V_1(x/t; U_L, U^+), & if\ \lambda_1(U_L) \le x/t \le \lambda_1(U^+) = 0, \\ V_1(x/t; U^{+s}, U), & if\ 0 \le x/t \le \lambda_1(U), \\ U, & if\ \lambda_1(U) < x/t < \ldots, \\ \ldots \end{cases} \tag{3.15}$$

On the other hand, if $U \in \mathcal{S}_1(U^{+s})$ such that $h^{s+} < h < h^{+s\#}$, i.e. $\sigma_1(U^{+s}, U) > 0$, then the third part of the solution can be $S_1(U^{+s}, U)$, i.e.

$$U_{exact}(x,t) = \begin{cases} U_L = (h_L, u_L, a_L), & \text{if } x/t < \lambda_1(U_L), \\ V_1(x/t; U_L, U^+), & \text{if } \lambda_1(U_L) \le x/t \le \lambda_1(U^+) = 0, \\ U^{+s}, & \text{if } 0 < x/t < \sigma_1(U^{+s}, U), \\ U, & \text{if } \sigma_1(U^{+s}, U) < x/t < \dots, \\ \dots \end{cases} \tag{3.16}$$

Thus, if $U \in \mathcal{W}_1(U^{+s})$ such that $0 < h < h^{+s\#}$ then first three parts of the Riemann solution are

$$R_1(U_L, U^+) \oplus W_3(U^+, U^{+s}) \oplus W_1(U^{+s}, U),$$

as Eqs. 3.15 or 3.16. Therefore, we call the set

$$\{U \in \mathcal{W}_1(U^{+s}) : \quad 0 < h < h^{+s\#}\} \tag{3.17}$$

as *the composite wave curve* $\mathcal{W}_{1.3.1}(U_L)$. Observe that $\mathcal{W}_{1.3.1}(U_L)$ is a part of the curve $\mathcal{W}_1(U^{+s})$.

If the curve $\mathcal{W}_2^B(U_R)$ intersects the curve $\mathcal{W}_{1.3.1}(U_L)$ at a point U_1, then the Riemann problem of Eqs. 1.1–1.2 admits a solution of the form

$$R_1(U_L, U^+) \oplus W_3(U^+, U^{+s}) \oplus W_1(U^{+s}, U_1) \oplus W_2(U_1, U_R). \tag{3.18}$$

Construction B2: The first part of the Riemann solution can be $R_1(U_L, U^+)$, as Eq. 3.13. For each level a between a_L and a_R, the second part of the Riemann solution can be $W_3(U^+, U^{+s})$, where $U^{+s} = (h^{+s}, u^{+s}, a)$. The third part of the Riemann solution can be $S_1(U^{+s}, U^{+s\#})$. The fourth part of the Riemann solution can be $W_3(U^{+s\#}, U^{+s\#b})$, where $U^{+s\#b} = (h^{+s\#b}, u^{+s\#b}, a_R)$. Since $W_3(U^+, U^{+s})$, $S_1(U^{+s}, U^{+s\#})$, $W_3(U^{+s\#}, U^{+s\#b})$ are discontinuity waves with same zero speed, first these parts of solution $R_1(U_L, U^+) \oplus W_3(U^+, U^{+s}) \oplus S_1(U^{+s}, U^{+s\#}) \oplus W_3(U^{+s\#}, U^{+s\#b})$ infer that

$$U_{exact}(x,t) = \begin{cases} U_L = (h_L, u_L, a_L), & \text{if } x/t < \lambda_1(U_L), \\ V_1(x/t; U_L, U^+), & \text{if } \lambda_1(U_L) \le x/t \le \lambda_1(U^+) = 0, \\ U^{+s\#b} = (h^{+s\#b}, u^{+s\#b}, a_R), & \text{if } 0 < x/t < \dots, \\ \dots \end{cases} \tag{3.19}$$

Therefore, we refer the set

$$\{U^{+s\#b} : \quad a \text{ varies between } a_L \text{ and } a_R\} \tag{3.20}$$

as *the composite wave curve* $\mathcal{W}_{1.3.1.3}(U_L)$.

If the curve $\mathcal{W}_2^B(U_R)$ intersects the curve $\mathcal{W}_{1.3.1.3}(U_L)$ at a point U_1, then the Riemann problem of Eqs. 1.1–1.2 admits a solution of the form

$$R_1(U_L, U^+) \oplus W_3(U^+, U^{+s}) \oplus S_1(U^{+s}, U^{+s\#}) \oplus W_3(U^{+s\#}, U_1 = U^{+s\#b}) \oplus W_2(U_1, U_R). \tag{3.21}$$

Construction B3: Take any $U_1 \in \mathcal{R}_1(U_L) \cap G_2$, the first part of the Riemann solution can be $R_1(U_L, U_1)$, i.e

$$U_{exact}(x,t) = \begin{cases} U_L = (h_L, u_L, a_L), & if\ x/t < \lambda_1(U_L), \\ V_1(x/t; U_L, U_1), & if\ \lambda_1(U_L) \le x/t \le \lambda_1(U_1), \\ U_1, & if\ \lambda_1(U_1) < x/t < \ldots, \\ \ldots \end{cases} \tag{3.22}$$

On the other hand, if we take $U_1 \in \mathcal{S}_1(U_L) \cap G_2$, the first part of the Riemann solution can be $S_1(U_L, U_1)$, i.e

$$U_{exact}(x,t) = \begin{cases} U_L = (h_L, u_L, a_L), & if\ x/t < \sigma_1(U_L, U_1), \\ U_1, & if\ \sigma_1(U_L, U_1) < x/t < \ldots, \\ \ldots \end{cases} \tag{3.23}$$

Thus, for any $U_1 \in \mathcal{W}_1(U_L) \cap G_2$, we have the first part of the Riemann solution $W_1(U_L, U_1)$. Then, the second part of the Riemann solution can be $W_3(U_1, U_1^b)$, where $U_1^b = (h_1^b, u_1^b, a_R)$, i.e.

$$U_{exact}(x,t) = \begin{cases} U_L = (h_L, u_L, a_L), & if\ x/t < \lambda_1(U_L), \\ Rare_1(x/t; U_L, U_1), & if\ \lambda_1(U_L) \le x/t \le \lambda_1(U_1), \\ U_1, & if\ \lambda_1(U_1) < x/t < 0, \\ U_1^b = (h_1^b, u_1^b, a_R), & if\ 0 < x/t < \ldots, \\ \ldots \end{cases} \tag{3.24}$$

or

$$U_{exact}(x,t) = \begin{cases} U_L = (h_L, u_L, a_L), & if\ x/t < \sigma_1(U_L, U_1), \\ U_1, & if\ \sigma_1(U_L, U_1) < x/t < 0, \\ U_1^b = (h_1^b, u_1^b, a_R), & if\ 0 < x/t < \ldots, \\ \ldots \end{cases} \tag{3.25}$$

Therefore, we refer the set

$$\{U_1^b : \quad U_1 \in \mathcal{W}_1(U_L) \cap G_2\} \tag{3.26}$$

as *the composite wave curve*, denoted by $\mathcal{W}_{1.3}^{caseB}(U_L)$. Observe that U^{-b} and U^{+b} be the two endpoints of this curve.

If the curve $\mathcal{W}_2^B(U_R)$ intersects the curve $\mathcal{W}_{1.3}^{caseB}(U_L)$ at a point U_2, then the Riemann problem of Eqs. 1.1–1.2 admits a solution of the form

$$W_1(U_L, U_1) \oplus W_3(U_1, U_2 = U_1^b) \oplus W_2(U_2, U_R). \tag{3.27}$$

Figure 2 illustrates the composite wave curves $\mathcal{W}_{1.3.1}(U_L)$, $\mathcal{W}_{1.3.1.3}(U_L)$ and $\mathcal{W}_{1.3}^{caseB}(U_L)$.

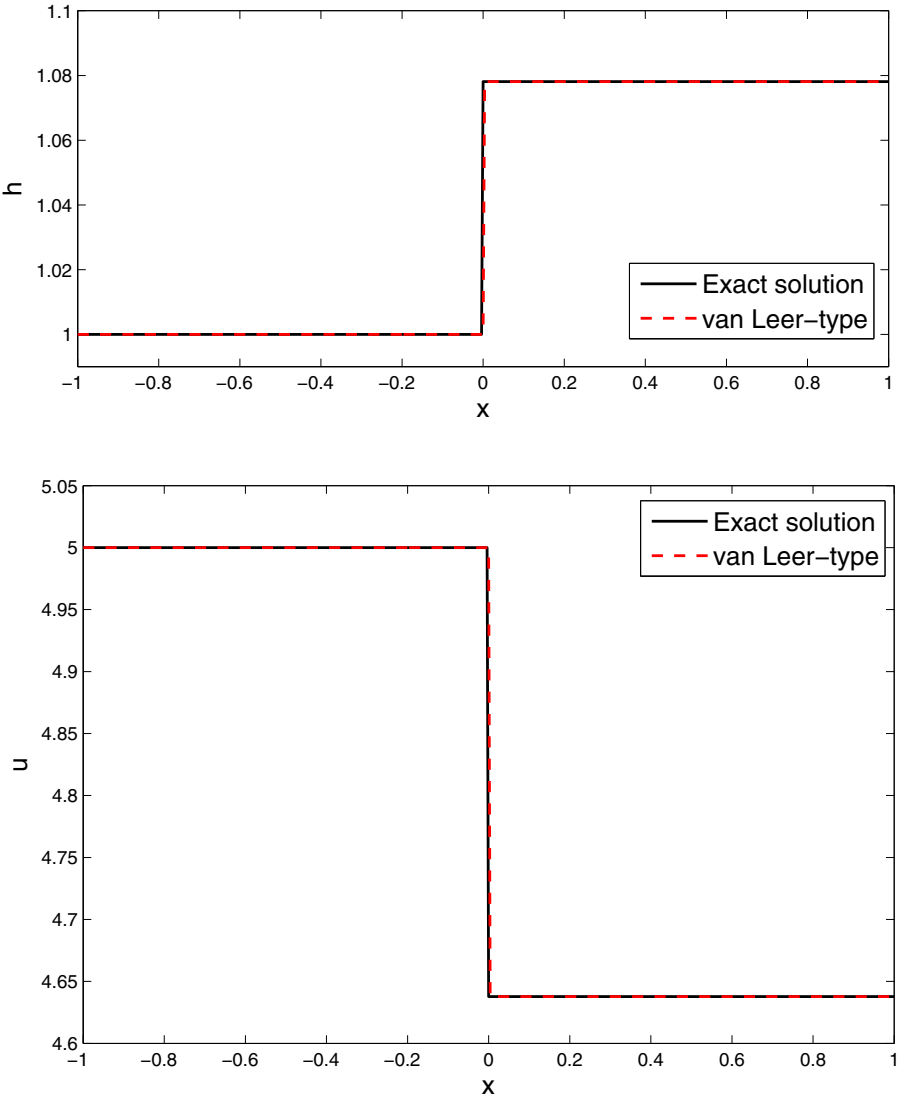

Fig. 3 Test 1: Well-balanced. Van Leer-type scheme can capture contact stationary wave exactly

4 A van Leer-type scheme

Relying on the constructions of Riemann solutions in the previous section, we are now in a position to build up a van Leer-type scheme for Eq. 1.1. Let us set

$$U := \begin{pmatrix} h \\ hu \end{pmatrix}, \quad F(U) := \begin{pmatrix} hu \\ h\left(u^2 + \frac{gh}{2}\right) \end{pmatrix}, \quad H(U) := \begin{pmatrix} 0 \\ -gh \end{pmatrix}. \tag{4.1}$$

Table 1 States that separate the elementary waves of the exact solution of the Riemann problem in Test 2: Construction A1

	U_1	U_2
h	0.59808364	1.27834878
u	4.68161945	2.32256983
a	1.8	1.8

Then, the system (1.1) can be written in form

$$\partial_t U + \partial_x F(U) = H(U)\partial_x a. \tag{4.2}$$

Accordingly, given the initial condition

$$U(x,0) = U_0(x), \quad x \in \mathbb{R}, \tag{4.3}$$

then, the discrete initial values $U^0 = (U_j^0)_{j\in\mathbb{Z}}$ are given by

$$U_j^0 := \frac{1}{\Delta x}\int_{x_{j-1/2}}^{x_{j+1/2}} U_0(x)dx, \quad j \in \mathbb{Z}. \tag{4.4}$$

4.1 The Godunov-type scheme revisited

Suppose $U^n = (U_j^n)_{j\in\mathbb{Z}}$ is known. We define the approximation $U^{n+1} = (U_j^{n+1})_{j\in\mathbb{Z}}$ of $U(.,t_{n+1})$ as follows:

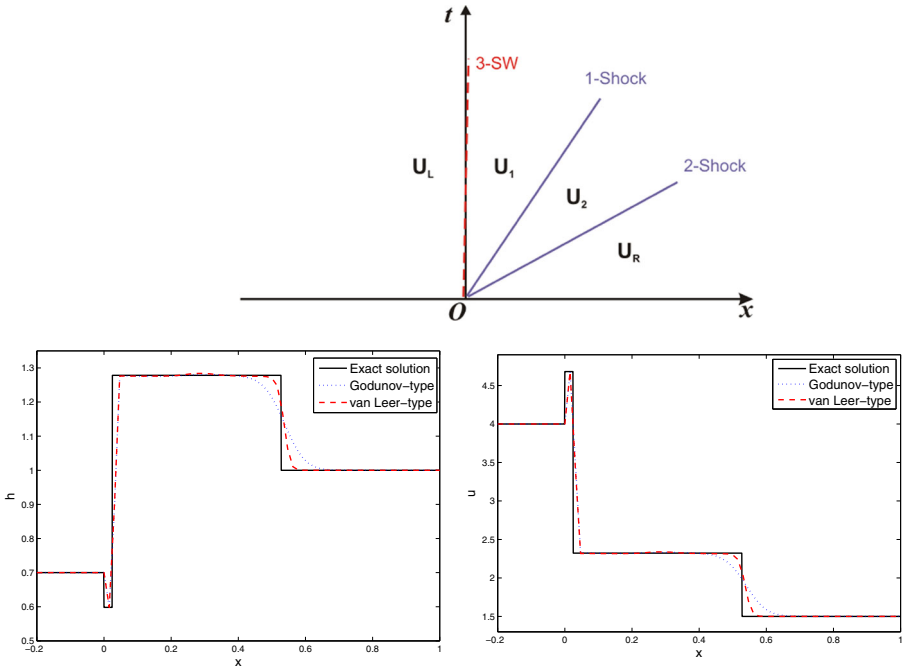

Fig. 4 Test 2: Construction A1. Exact solution and approximate solutions for the mesh size $h = 1/128$ corresponding to the Godunov-type scheme and the van Leer-type scheme

(i) We extend the sequence U^n as a piecewise constant function $U_{p.con}(., t_n)$ defined by

$$U_{p.con}(x, t_n) = U_j^n, \quad x_{j-1/2} < x < x_{j+1/2}, \quad j \in \mathbb{Z}. \tag{4.5}$$

(ii) We solve the local Riemann problems for Eq. 4.2 with the initial condition

$$U(x, 0) = U_{p.con}(x, t_n), \tag{4.6}$$

to find the solution $U(., \Delta t)$. This solution is obtained by solving a juxtaposition of local Riemann problems, so

$$U(x, t) = U_{exact}\Big(\frac{x - x_{j+1/2}}{t}; U_j^n, U_{j+1}^n\Big), \quad x_j < x < x_{j+1}, \quad j \in \mathbb{Z}, \tag{4.7}$$

where $U_{exact}\Big(\frac{x}{t}; U_L, U_R\Big)$ denote the exact solution of the Riemann problem for Eq. 4.2 corresponding to the Riemann data (U_L, U_R).

(iii) We project ($\mathbb{L}^2$-projection) the exact solution $U(., \Delta t)$ onto the piecewise constant functions, i.e.

$$U_j^{n+1} := \frac{1}{\Delta x}\int_{x_{j-1/2}}^{x_{j+1/2}} U(x, \Delta t)dx. \tag{4.8}$$

Provided we assume the C.F.L. condition

$$\frac{\Delta t}{\Delta x}\max\{|\lambda_k(U_j^n)| : k = 1, 2\} \leq \frac{1}{2}, \tag{4.9}$$

so that the waves issued from the points $x_{j-1/2}$ and $x_{j+1/2}$ do not interact. Since the a-component is constant in each interval $(x_{j-1/2}, x_{j+1/2})$, then the right-hand side of Eq. 4.2 vanishes. Thus, the Godunov-type scheme is

$$U_j^{n+1} = U_j^n - \frac{\Delta t}{\Delta x}\Big(F(U_{exact}(0-; U_j^n, U_{j+1}^n)) - F(U_{exact}(0+; U_{j-1}^n, U_j^n))\Big). \tag{4.10}$$

To complete the Godunov-type scheme (4.10), we will specify the values

$$\begin{aligned} U_{left} &:= U_{exact}\Big(0-; U_L, U_R\Big), \\ U_{right} &:= U_{exact}\Big(0+; U_L, U_R\Big), \end{aligned} \tag{4.11}$$

as follows.

Construction	U_{left}	U_{right}
A1(3.5)	U_L	U^s
A2(3.8)	U_L	$U^{s\#b}$
A3(3.12)	U_1	U_2
B1(3.18)	U^+	U^{+s}
B2(3.21)	U^+	$U^{+s\#b}$
3(3.27)	U_1	U_2

(4.12)

Table 2 Errors and orders of convergence for Test 2: Construction A1

	Godunov-type scheme			van Leer-type scheme		
N	L^1-error	L^1-relative error	Order	L^1-error	L^1-relative error	Order
128	0.0767	0.00980	–	0.0505	0.00646	–
256	0.0545	0.00696	0.49	0.0398	0.00508	0.35
512	0.0219	0.00279	1.32	0.0153	0.00196	1.38
1024	0.0097	0.00124	1.17	0.0073	0.00094	1.06

4.2 Building a van Leer-type scheme

Suppose $U^n = (U_j^n)_{j\in\mathbb{Z}}$ at the time t_n is known. We define the approximation $U^{n+1} = (U_j^{n+1})_{j\in\mathbb{Z}}$ of $U(\cdot, t_{n+1})$ as follows:

(i) From the sequence U^n, we construct a piecewise linear function $U_{p.lin}(\cdot, t_n)$ defined by

$$U_{p.lin}(x, t_n) = U_j^n + \frac{S_j^n}{\Delta x}(x - x_j), \quad x_{j-1/2} < x < x_{j+1/2}, \quad j \in \mathbb{Z}, \tag{4.13}$$

where the slopes S_j^n are defined by

$$\begin{aligned} S_j^n &= (U_{j+1}^n - U_j^n)\Phi(\theta_j^n), \\ \theta_j^n &= \frac{U_j^n - U_{j-1}^n}{U_{j+1}^n - U_j^n}, \\ \Phi(\theta) &= \frac{|\theta| + \theta}{1 + |\theta|}, \quad \textit{the van Leer's limiter function}. \end{aligned} \tag{4.14}$$

(ii) We solve the Cauchy problem for Eq. 4.2 with the initial condition

$$U(x, 0) = U_{p.lin}(x, t_n), \tag{4.15}$$

to find the solution $U(\cdot, \Delta t)$.

(iii) We project (in the sense of $\mathbb{L}^2$) the solution $U(\cdot, \Delta t)$ onto the piecewise constant functions, i.e., we set

$$U_j^{n+1} := \frac{1}{\Delta x}\int_{x_{j-1/2}}^{x_{j+1/2}} U(x, \Delta t)dx. \tag{4.16}$$

Table 3 States that separate the elementary waves of the exact solution of the Riemann problem in Test 3: Construction A2

	U_1	U_2	U_3
h	0.83623250	2.08708713	2.24123887
u	5.97919835	2.39568340	2.23090902
a	2.61525664	2.61525664	2.5

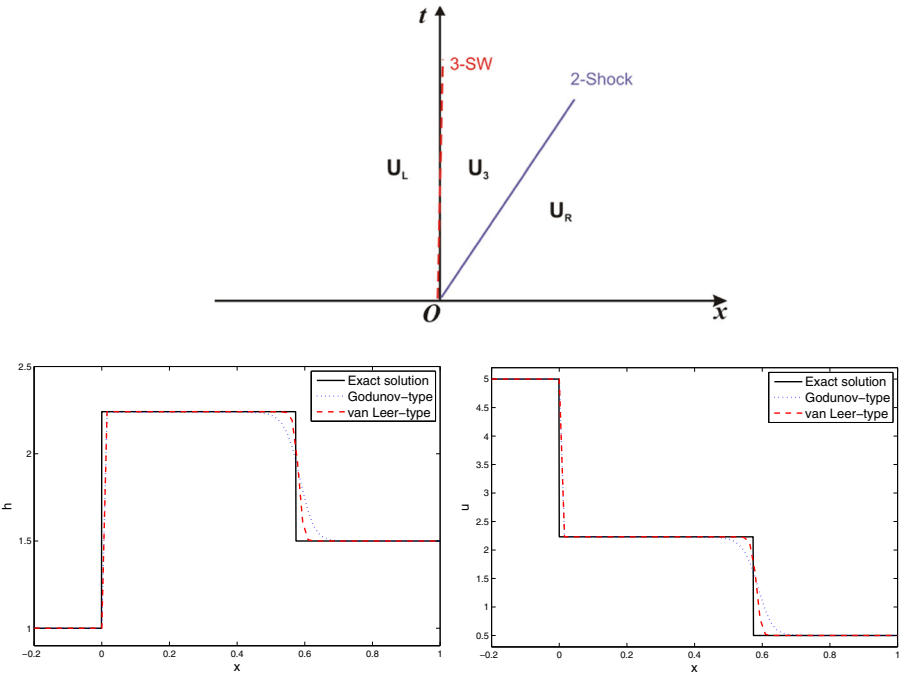

Fig. 5 Test 3: Construction A2. Exact solution and approximate solutions for the mesh size $h = 1/128$ corresponding to the Godunov-type scheme and the van Leer-type scheme

Provided we assume some C.F.L. condition so that the waves issued from the points $x_{j-1/2}$ and $x_{j+1/2}$ do not interact, the solution is obtained by juxtaposition of local Riemann problems

$$\frac{\Delta t}{\Delta x}\max\{|\lambda_k(U_j^n)| : k = 1, 2\} \le \frac{1}{2}. \tag{4.17}$$

In order to derive a more explicit form of the scheme, we integrate the Eq. 4.2 over the rectangle $(x_{j-1/2}, x_{j+1/2}) \times (0, \Delta t)$. Since a is constant on $(x_{j-1/2}, x_{j+1/2})$, we obtain

$$\int_{x_{j-1/2}}^{x_{j+1/2}} (U(x, \Delta x) - U(x, 0))dx + \int_0^{\Delta t} \Big(F(U(x_{j+1/2} - 0, t)) - F(U(x_{j-1/2} + 0, t))\Big)dt = 0. \tag{4.18}$$

Using Eqs. 4.13, 4.15 and 4.16, we get

$$\Delta x(U_j^{n+1} - U_j^n) + \int_0^{\Delta t} \Big(F(U(x_{j+1/2} - 0, t)) - F(U(x_{j-1/2} + 0, t))\Big)dt = 0. \tag{4.19}$$

Using the midpoint rule, we write

$$\frac{1}{\Delta t}\int_0^{\Delta t} F(U(x_{j+1/2} - 0, t))dt = F(U(x_{j+1/2} - 0, \Delta t/2)) + O(\Delta t^2). \tag{4.20}$$

Table 4 Errors and orders of convergence for Test 3: Construction A2

	Godunov-type scheme			**van Leer-type scheme**		
N	L^1-error	L^1-relative error	Order	L^1-error	L^1-relative error	Order
128	0.0748	0.00796	–	0.0211	0.00225	–
256	0.0402	0.00427	0.90	0.0163	0.00173	0.37
512	0.0200	0.00212	1.01	0.0053	0.00056	1.63
1024	0.0099	0.00106	1.01	0.0035	0.00037	0.59

For approximating $F(U(x_{j+1/2}-0,\Delta t/2))$, we use a predictor-corrector scheme. First, we define the updated values $U^{n+1/2}_{j+1/2,\pm}$ at time $t_n+\Delta t/2$ by

$$\begin{aligned} U^{n+1/2}_{j+1/2,-} &= U^n_{j+1/2,-} - \frac{\Delta t}{2\Delta x}(F(U^n_{j+1/2,-}) - F(U^n_{j-1/2,+})),\\ U^{n+1/2}_{j+1/2,+} &= U^n_{j+1/2,+} - \frac{\Delta t}{2\Delta x}(F(U^n_{j+3/2,-}) - F(U^n_{j+1/2,+})), \end{aligned} \tag{4.21}$$

where

$$\begin{aligned} U^n_{j+1/2,-} &= U_{p.lin}(x_{j+1/2}-0) = U^n_j + \frac{1}{2}S^n_j,\\ U^n_{j+1/2,+} &= U_{p.lin}(x_{j+1/2}+0) = U^n_{j+1} - \frac{1}{2}S^n_j, \end{aligned} \tag{4.22}$$

see [14], for example. Second, we solve the Riemann problem of Eq. 4.2 at the point $x_{j+1/2}$ with piecewise constant initial data $U^{n+1/2}_{j+1/2,\pm}$, whose solution is noted as usual

$$U_{exact}\Big(\frac{x-x_{j+1/2}}{t}; U^{n+1/2}_{j+1/2,-}, U^{n+1/2}_{j+1/2,+}\Big).$$

Third, we replace $U(x_{j+1/2}\pm 0,\Delta t/2)$ by

$$U_{exact}\Big(0\pm; U^{n+1/2}_{j+1/2,-}, U^{n+1/2}_{j+1/2,+}\Big).$$

Thus, the scheme (4.19) becomes

$$U^{n+1}_j = U^n_j - \frac{\Delta t}{\Delta x}\Big(F(U_{exact}(0-, U^{n+1/2}_{j+1/2,-}, U^{n+1/2}_{j+1/2,+})) - F(U_{exact}(0+, U^{n+1/2}_{j-1/2,-}, U^{n+1/2}_{j-1/2,+}))\Big). \tag{4.23}$$

The scheme (4.23) is capable of capturing stationary waves exactly. This means that for any stationary wave, it holds that

$$U^{n+1}_j = U^n_j, \quad j\in\mathbb{Z}, \quad n=0,1,2,\ldots \tag{4.24}$$

Therefore, it is a *well-balanced scheme*. To see this, we first suppose that U^n corresponds to a stationary wave. From Eq. 4.14, we imply

$$S^n_j = 0, \quad j\in\mathbb{Z}.$$

Table 5 States that separate the elementary waves of the exact solution of the Riemann problem in Test 4: Construction A3

	U_1	U_2
h	2.78773441	3.50171819
u	3.38414574	2.69413443
a	2.0	1.5

Then, we get from Eqs. 4.21, 4.22

$$U^{n+1/2}_{j+1/2,-} = U^{n}_{j+1/2,-} = U^{n}_{j},$$
$$U^{n+1/2}_{j+1/2,+} = U^{n}_{j+1/2,+} = U^{n}_{j+1}.$$

Therefore, it holds that

$$U_{exact}\left(0-; U^{n+1/2}_{j+1/2,-}, U^{n+1/2}_{j+1/2,+}\right) = U^{n}_{j} = U_{exact}\left(0+; U^{n+1/2}_{j-1/2,-}, U^{n+1/2}_{j-1/2,+}\right),$$

which yield (4.24).

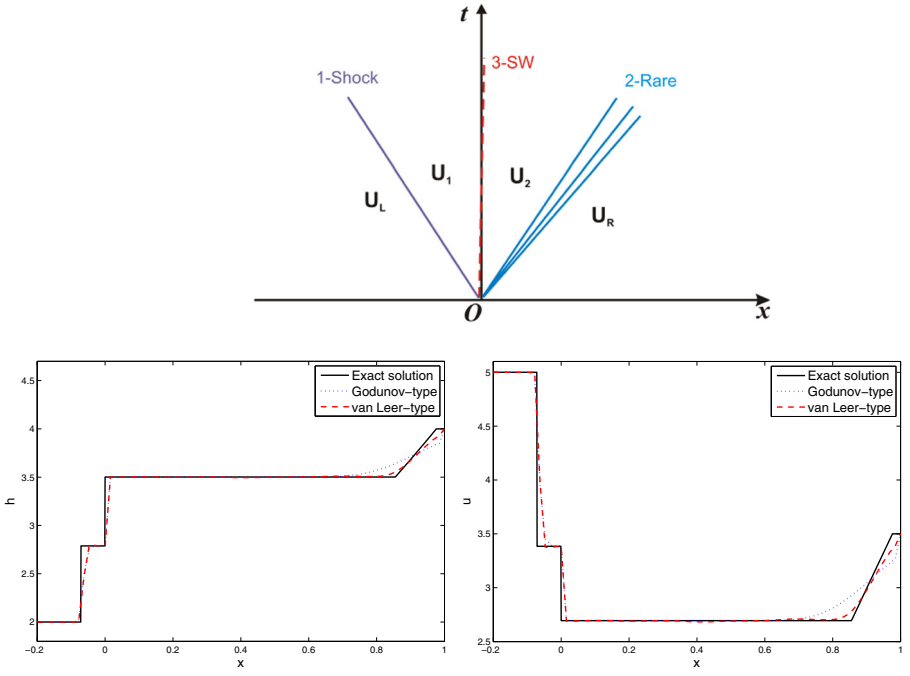

Fig. 6 Test 4: Construction A3. Exact solution and approximate solutions for the mesh size $h = 1/128$ corresponding to the Godunov-type scheme and the van Leer-type scheme

Table 6 Errors and orders of convergence for Test 4: Construction A3

	Godunov-type scheme			**van Leer-type scheme**		
N	L^1-error	L^1-relative error	Order	L^1-error	L^1-relative error	Order
128	0.0953	0.00719	–	0.0573	0.00433	–
256	0.0511	0.00386	0.90	0.0184	0.00139	1.64
512	0.0370	0.00280	0.46	0.0132	0.00100	0.48
1024	0.0256	0.00193	0.54	0.0089	0.00067	0.57

5 Numerical experiments

This section is devoted to numerical tests by using MATLAB, which demonstrate the advantages of our scheme (4.23). For each test, we compare the numerical solution U_h with the corresponding exact solution U. By taking

$$g = 9.8,$$

we plot the solutions U_h and U for

$$x \in [-1, 1], \quad t = 0.1.$$

5.1 Test 1: Well-balanced property

Let the Riemann data be given by

$$\begin{array}{ccc} & U_L \in G_1 & U_R \in G_1 \\ h & 1.0 & 1.07809232 \\ u & 5.0 & 4.63782175 \\ a & 3.0 & 3.1 \end{array} \tag{5.1}$$

It is not difficult to check that the initial data (5.1) satisfies the jump relations (2.12). Therefore, the solution is just a stationary wave from U_L to U_R. Figure 3 displays an exact contact stationary wave and its approximation with 500 mesh points by the van Leer-type scheme (4.23). This figure shows that the van Leer-type scheme (4.23) can capture contact stationary solutions, so it is well-balanced.

Table 7 States that separate the elementary waves of the exact solution of the Riemann problem in Test 5: Construction B1

	U^+	U_1	U_2
h	0.77374106	0.58589019	0.64142927
u	2.75366345	3.63655599	3.41438207
a	1.1	1.0	1.0

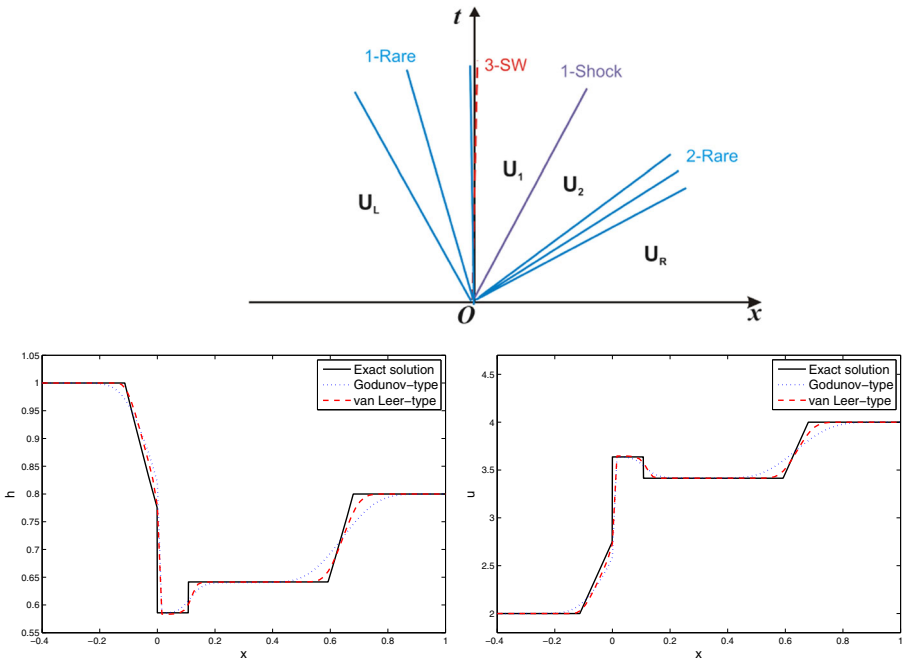

Fig. 7 Test 5: Construction B1. Exact solution and approximate solutions for the mesh size $h = 1/128$ corresponding to the Godunov-type scheme and the van Leer-type scheme

5.2 Test 2: Construction A1

In this test we approximate a Riemann solution of Construction A1. Precisely, let the Riemann data be given by

$$\begin{array}{lll} & U_L \in G_1 & U_R \in G_2 \\ h & 0.7 & 1.0 \\ u & 4.0 & 1.5 \\ a & 2.0 & 1.8 \end{array} \tag{5.2}$$

It holds that the initial data (5.2) satisfies the Construction A1. Therefore, acccording to Eq. 3.5, the exact solution is a stationary wave from U_L to U_1, followed by a $1-$shock wave from U_1 to U_2, then followed by a $2-$shock wave from U_2 to U_R, where U_1, U_2 are reported in Table 1, see the top of Fig. 4. The rest of Fig. 4 displays the exact solution and its approximate solutions for the mesh size $h = 1/128$ corresponding to the Godunov-type scheme and the van Leer-type scheme. The errors, orders of convergence are reported by Table 2. Moreover, Table 2 shows that the accuracy of the van Leer-type scheme is better than the Godunov-type scheme while the order of the van Leer-type scheme seems equal to the one of the Godunov-type scheme.

Table 8 Errors and orders of convergence for Test 5: Construction B1

	Godunov-type scheme			**van Leer-type scheme**		
N	L^1-error	L^1-relative error	Order	L^1-error	L^1-relative error	Order
128	0.0597	0.00810	–	0.0230	0.00312	–
256	0.0401	0.00543	0.58	0.0117	0.00158	0.98
512	0.0262	0.00356	0.61	0.0057	0.00078	1.03
1024	0.0167	0.00227	0.65	0.0028	0.00038	1.05

5.3 Test 3: Construction A2

In this test we approximate a Riemann solution of Construction A2. Precisely, we consider the Riemann problem for Eqs. 1.1–1.2 with the initial data of the form

$$\begin{array}{lll} & U_L \in G_1 & U_R \in G_2 \\ h & 1.0 & 1.5 \\ u & 5.0 & 0.5 \\ a & 3.0 & 2.5 \end{array} \tag{5.3}$$

It holds that the initial data (5.3) satisfies Construction A2. According to Eq. 3.8, the exact solution is a stationary wave from U_L to U_1, followed by a $1-$shock which has zero speed from U_1 to U_2, followed again by a stationary from U_2 to U_3, then followed by a $2-$shock from U_3 to U_R, where U_1, U_2, U_3 are reported in Table 3, see the top of Fig. 5. The rest of Fig. 5 displays the exact solution and its approximate solutions for the mesh size $h = 1/128$ corresponding to the Godunov-type scheme and the van Leer-type scheme. This figure illustrates good approximations to the exact solution. The errors and order of convergence for Test 3 are reported in the Table 4, where one can see that the accuracy of the van Leer-type scheme is better than the Godunov-type scheme while the order of the van Leer-type scheme looks like equal to the one of the Godunov-type scheme. Note that second-order schemes may have the order of accuracy less than 1 when approximating shock waves and therefore solutions containing shock waves even for the conservative systems such as the usual gas dynamics equations, see [10].

Table 9 States that separate the elementary waves of the exact solution of the Riemann problem in Test 6: Construction B2

	U^+	U_1	U_2	U_3
h	0.77374106	0.52701539	1.08828154	1.47743632
u	2.75366345	4.04280884	1.95778610	1.44210782
a	1.5	1.29970317	1.29970317	1.0

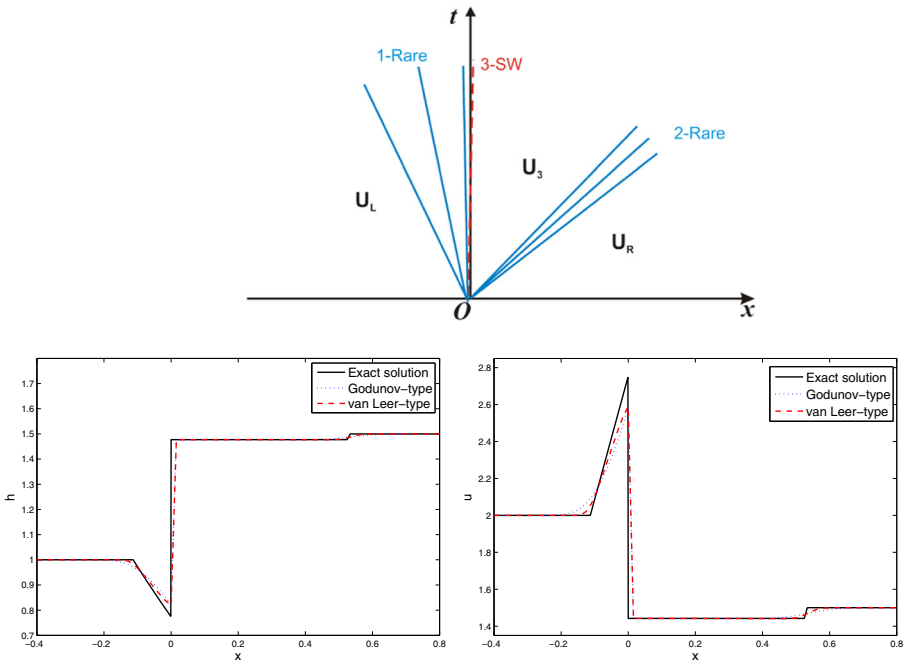

Fig. 8 Test 6: Construction B2. Exact solution and approximate solutions for the mesh size $h = 1/128$ corresponding to the Godunov-type scheme and the van Leer-type scheme

5.4 Test 4: Construction A3

Let the Riemann data be given by

$$\begin{array}{lll} & U_L \in G_1 & U_R \in G_2 \\ h & 2.0 & 4.0 \\ u & 5.0 & 3.5 \\ a & 2.0 & 1.5 \end{array} \tag{5.4}$$

It holds that the initial data (5.4) satisfies the Construction A3. According to Eq. 3.12, the exact solution is a $1-$shock wave from U_L to U_1, followed by a stationary wave from U_1 to U_2, then followed by a $2-$rarefaction wave from U_2 to U_R, where U_1, U_2 are reported in Table 5, see the top of Fig. 6. The rest of Fig. 6 displays the exact solution and its approximate solutions for the mesh size $h = 1/128$ corresponding to the Godunov-type scheme and the van Leer-type scheme. One can see from this figure that the approximate solutions are closed to the exact solution. The errors, orders of convergence are reported by Table 6. Moreover, Table 6 shows that the van Leer-type scheme has a better accuracy than the Godunov-type scheme while the order of the van Leer-type scheme seems equal to the one of the Godunov-type scheme.

Table 10 Errors and orders of convergence for Test 6: Construction B2

	Godunov-type scheme			**van Leer-type scheme**		
N	L^1-error	L^1-relative error	Order	L^1-error	L^1-relative error	Order
128	0.0173	0.00290	–	0.0116	0.00193	–
256	0.0116	0.00193	0.58	0.0058	0.00098	0.98
512	0.0076	0.00128	0.60	0.0029	0.00049	0.99
1024	0.0049	0.00082	0.63	0.0015	0.00025	1.00

5.5 Test 5: Construction B1

In this test we approximate a Riemann solution of Construction B1. Precisely, let the Riemann data be given by

$$\begin{array}{lll} & U_L \in G_2 & U_R \in G_1 \\ h & 1.0 & 0.8 \\ u & 2.0 & 4.0 \\ a & 1.1 & 1.0 \end{array} \tag{5.5}$$

It holds that the initial data (5.5) satisfies the Construction B1. Therefore, according to Eq. 3.18, the exact solution is a $1-$rarefaction wave from U_L to U^+, followed by a stationary wave from U^+ to U_1, followed by a $1-$shock wave from U_1 to U_2, then followed by a $2-$rarefaction wave from U_2 to U_R, where U^+, U_1, U_2 are reported in Table 7, see the top of Fig. 7. The rest of Fig. 7 displays the exact solution and its approximate solutions for the mesh size $h = 1/128$ corresponding to the Godunov-type scheme and the van Leer-type scheme. We can see from this figure that the approximate solutions are closed to the exact solution. The errors, orders of convergence are reported by Table 8. Moreover, Table 8 shows that the accuracy and the order of the van Leer-type scheme are better than the Godunov-type scheme.

5.6 Test 6: Construction B2

In this test we approximate a Riemann solution of Construction B2. Precisely, we consider the Riemann problem for Eqs. 1.1–1.2 with the initial data of the form

$$\begin{array}{lll} & U_L \in G_2 & U_R \in G_2 \\ h & 1.0 & 1.5 \\ u & 2.0 & 1.5 \\ a & 1.5 & 1.0 \end{array} \tag{5.6}$$

Table 11 States that separate the elementary waves of the exact solution of the Riemann problem in Test 7: Construction B3

	U_1	U_2
h	1.48876884	1.99695818
u	0.60112084	0.44814658
a	1.5	1.0

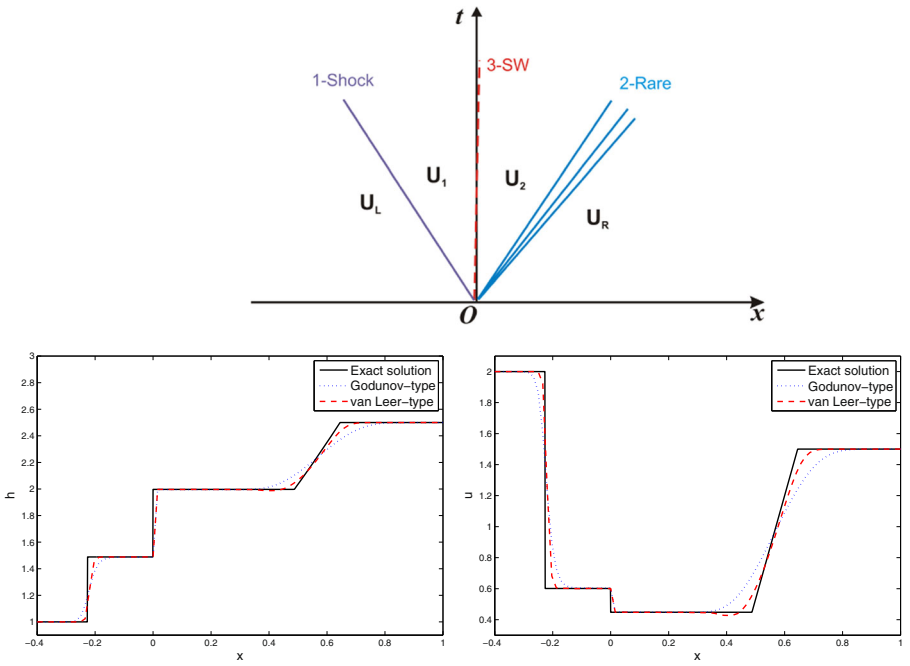

Fig. 9 Test 7: Construction B3. Exact solution and approximate solutions for the mesh size $h = 1/128$ corresponding to the Godunov-type scheme and the van Leer-type scheme

It holds that the initial data (5.6) satisfies Construction B2. According to Eq. 3.21, the exact solution is a $1-$rarefaction wave from U_L to U^+, followed by a stationary wave from U^+ to U_1, followed by a $1-$shock which has zero speed from U_1 to U_2, followed again by a stationary from U_2 to U_3, then followed by a $2-$rarefaction from U_3 to U_R, where U^+, U_1, U_2, U_3 are reported in Table 9, see the top of Fig. 8. The rest of Fig. 8 displays the exact solution and its approximate solutions for the mesh size $h = 1/128$ corresponding to the Godunov-type scheme and the van Leer-type scheme. This figure illustrates good approximations to the exact solution. The errors and orders of convergence for this test are reported in the Table 10, where one can see that the accuracy and the order of the van Leer-type scheme are better than the Godunov-type scheme.

5.7 Test 7: Construction B3

Let the Riemann data be given by

$$\begin{array}{lll} & U_L \in G_2 & U_R \in G_2 \\ h & 1.0 & 2.5 \\ u & 2.0 & 1.5 \\ a & 1.5 & 1.0 \end{array} \tag{5.7}$$

Table 12 Errors and orders of convergence for Test 7: Construction B3

	Godunov-type scheme			**van Leer-type scheme**		
N	L^1-error	L^1-relative error	Order	L^1-error	L^1-relative error	Order
128	0.1121	0.01894	–	0.0496	0.00838	–
256	0.0709	0.01198	0.66	0.0306	0.00517	0.70
512	0.0403	0.00681	0.82	0.0120	0.00202	1.35
1024	0.0235	0.00397	0.78	0.0055	0.00094	1.11

It holds that the initial data (5.7) satisfies the Construction B3. According to Eq. 3.27, the exact solution is a $1-$shock wave from U_L to U_1, followed by a stationary wave from U_1 to U_2, then followed by a $2-$rarefaction wave from U_2 to U_R, where U_1, U_2 are reported in Table 11, see the top of Fig. 9. The rest of Fig. 9 displays the exact solution and its approximate solutions for the mesh size $h = 1/128$ corresponding to the Godunov-type scheme and the van Leer-type scheme. One can see from this figure that the approximate solutions are closed to the exact solution. The errors, orders of convergence are reported by Table 12. Moreover, Table 12 shows that the accuracy and the order of the van Leer-type scheme are better than the Godunov-type scheme.

6 Conclusions

Nonconservative systems often cause lots of inconvenience for numerical approximations. The resonance problem is a typically difficult one in this kind of systems when wave speeds associated with different characteristic fields coincide. The significant gain of this work is the success in numerical treatments for the resonance problem by constructing a well-balanced van Leer-type numerical scheme for the shallow water equations with variable topography (1.1). Moreover, a Godunov-type scheme for Eq. 1.1 is also revisited. These schemes are constructed based on exact solutions of local Riemann problems at each grid cell. The two methods are shown to be well-balanced, since they can capture exactly stationary contact discontinuity waves. Numerical tests are conducted for data in all the cases: data belong to the subcritical region, supercritical region, or both. Tests are also made for the resonant cases where the exact Riemann solutions contain coinciding waves. All of these tests show that both schemes can give approximate solutions which are convergent to the exact solutions. Furthermore, the van Leer-type scheme can give a better accuracy than the Godunov-type scheme-as expected. This work motivates for further developments for numerical treatments of the resonance problem in more complicated systems such as multi-phase flow models.

Acknowledgments The authors are grateful to the reviewers for their very constructive comments and fruitful discussions. This research is funded by Vietnam National University HoChiMinh City (VNU-HCM) under grant number B2015-28-02.

References

1. Ambroso, A., Chalons, C., Coquel, F., Galié, T.: Relaxation and numerical approximation of a two-fluid two-pressure diphasic model. Math. Mod. Numer. Anal. **43**, 1063–1097 (2009)
2. Ambroso, A., Chalons, C., Raviart, P.-A.: A Godunov-type method for the seven-equation model of compressible two-phase flow. Comput. Fluids **54**, 67–91 (2012)
3. Audusse, E., Bouchut, F., Bristeau, M.-O., Klein, R., Perthame, B.: A fast and stable well-balanced scheme with hydrostatic reconstruction for shallow water flows. SIAM J. Sci Comput. **25**, 2050–2065 (2004)
4. Baudin, M., Coquel, F., Tran, Q.-H.: A semi-implicit relaxation scheme for modeling two-phase flow in a pipeline. SIAM J. Sci. Comput. **27**, 914–936 (2005)
5. Botchorishvili, R., Perthame, B., Vasseur, A.: Equilibrium schemes for scalar conservation laws with stiff sources. Math. Comput. **72**, 131–157 (2003)
6. Botchorishvili, R., Pironneau, O.: Finite volume schemes with equilibrium type discretization of source terms for scalar conservation laws. J. Comput. Phys. **187**, 391–427 (2003)
7. Chinnayya, A., LeRoux, A.-Y., Seguin, N.: A well-balanced numerical scheme for the approximation of the shallow water equations with topography: the resonance phenomenon. Int. J. Finite **1**(4), (2004)
8. Castro, C.E., Toro, E.F.: A Riemann solver and upwind methods for a two-phase flow model in non-conservative form. Internat. J. Numer. Methods Fluids **50**, 275–307 (2006)
9. Cuong, D.H., Thanh, M.D.: A Godunov-type scheme for the isentropic model of a fluid flow in a nozzle with variable cross-section. Appl. Math. Comput. **256**, 602–629
10. Coquel, F., Helluy, P., Schneider, J.: Second-order entropy diminishing scheme for the Euler equations. Int. J. Num. Meth. Fluids **50**, 1029–1061 (2006)
11. Coquel, F., Hérard, J.-M., Saleh, K., Seguin, N.: Two properties of two-velocity two-pressure models for two-phase flows. Commun. Math. Sci. **12**, 593–600 (2014)
12. Dal Maso, G., LeFloch, P.G., Murat, F.: Definition and weak stability of nonconservative products. J. Math. Pures Appl. **74**, 483–548 (1995)
13. Gallardo, J.M., Parés, C., Castro, M.: On a well-balanced high-order finite volume scheme for shallow water equations with topography and dry areas. J. Comput. Phys. **227**, 574–601 (2007)
14. Godlewski, E., Raviart, P.A.: Numerical approximation of hyperbolic systems of conservation laws. Springer, New York (1996)
15. Greenberg, J.M., Leroux, A.Y.: A well-balanced scheme for the numerical processing of source terms in hyperbolic equations. SIAM J. Numer. Anal. **33**, 1–16 (1996)
16. Goatin, P., LeFloch, P.G.: The Riemann problem for a class of resonant nonlinear systems of balance laws. Ann. Inst. H. Poincar Anal. NonLinéaire **21**, 881–902 (2004)
17. Gallouët, T., Hérard, J.-M., Seguin, N.: Numerical modeling of two-phase flows using the two-fluid two-pressure approach. Math. Models Methods Appl. Sci. **14**, 663–700 (2004)
18. Hou, T.Y., LeFloch, P.: Why nonconservative schemes converge to wrong solutions. Error Anal. Math. of Comput. **62**, 497–530 (1994)
19. Isaacson, E., Temple, B.: Nonlinear resonance in systems of conservation laws. SIAM J. Appl. Math. **52**, 1260–1278 (1992)
20. Isaacson, E., Temple, B.: Convergence of the 22 Godunov method for a general resonant nonlinear balance law. SIAM J. Appl. Math. **55**, 625–640 (1995)
21. Keyfitz, B.L., Sander, R., Sever, M.: Lack of hyperbolicity in the two-fluid model for two-phase incompressible flow. Discret. Cont. Dyn. Sys.-Ser. B **3**, 541–563 (2003)
22. Kröner, D., Thanh, M.D.: Numerical solutions to compressible flows in a nozzle with variable cross-section. SIAM J. Numer. Anal. **43**, 796–824 (2005)
23. Kröner, D., LeFloch, P.G., Thanh, M.D.: The minimum entropy principle for fluid flows in a nozzle with discntinuous crosssection. Math. Mod. Numer. Anal. **42**, 425–442 (2008)
24. LeFloch, P.G.: Entropy weak solutions to nonlinear hyperbolic systems in nonconservative form. Com. Partial. Diff. Eqs. **13**, 669–727 (1988)
25. LeFloch, P.G.: Shock waves for nonlinear hyperbolic systems in nonconservative form, Institute for Math. and its Appl. Minneapolis, Preprint, # 593 (1989)
26. LeFloch, P.G., Thanh, M.D.: The Riemann problem for fluid flows in a nozzle with discontinuous cross-section. Comm. Math. Sci. **1**, 763–797 (2003)
27. LeFloch, P.G., Thanh, M.D.: The Riemann problem for shallow water equations with discontinuous topography. Comm. Math. Sci. **5**, 865–885 (2007)

28. LeFloch, P.G., Thanh, M.D.: A Godunov-type method for the shallow water equations with variable topography in the resonant regime. J. Comput. Phys. **230**, 7631–7660 (2011)
29. Marchesin, D., Paes-Leme, P.J.: A Riemann problem in gas dynamics with bifurcation. Hyperbolic partial differential equations III. Comput. Math. Appl. (Part A) **12**, 433–455 (1986)
30. Rosatti, G., Begnudelli, L.: The Riemann Problem for the one-dimensional, free-surface shallow water equations with a bed step: theoretical analysis and numerical simulations. J. Comput. Phys. **229**, 760–787 (2010)
31. Schwendeman, D.W., Wahle, C.W., Kapila, A.K.: The Riemann problem and a high-resolution Godunov method for a model of compressible two-phase flow. J. Comput. Phys. **212**, 490–526 (2006)
32. Saurel, R., Abgrall, R.: A multi-phase Godunov method for compressible multifluid and multiphase flows. J. Comput. Phys. **150**, 425–467 (1999)
33. Tian, B., Toro, E.F., Castro, C.E.: A path-conservative method for a five-equation model of two-phase flow with an HLLC-type Riemann solver. Comput. Fluids **46**, 122–132 (2011)
34. Thanh, M.D., phase decomposition approach, A.: the Riemann problem for a model of two-phase flows. J. Math. Anal Appl. **418**, 569–594 (2014)
35. Thanh, M.D.: The Riemann problem for a non-isentropic fluid in a nozzle with discontinuous cross-sectional area. SIAM J. Appl. Math. **69**, 1501–1519 (2009)
36. Thanh, M.D., Cuong, D.H.: Existence of solutions to the Riemann problem for a model of two-phase flows. Elect. J. Diff. Eqs. **2015**(32), 1–18 (2015)